

DEAD REGION TIME EVOLUTION AND AFTERPULSES DEVELOPMENT IN SQS

E.P. de Lima, M. Salete S.C.P. Leite, A.J.P.L. Policarpo and M.A.F. Alves

Departamento de Física, Universidade de Coimbra, 3000 Coimbra, Portugal

Abstract

The dead length, δ , for $t \lesssim 20 \mu\text{s}$ is well approximated by $\delta = \delta_0 \exp(-t/\tau)$ for mixtures of argon-isobutane with benzene or TEA. δ_0 varies in an approximate linear way with the streamer charge and the systematics of τ regarding the high voltage is also presented.

Afterpulses are associated not only with wall effects but also with photoionization in the gas mixture itself. Interpretation of the data is attempted.

1. Introduction

Self-quenching streamers (SQS) feature characteristics, that suitably developed, could lead to widespread applications, as radiation detectors, in many fields of physics. One of them is its localization properties and associated with it the short dead time. The dead length of the wire related to each streamer decreases with time; this evolution is of instrumental interest and may also contribute to clarify some general features of these processes.

Another important characteristic is the stability of operation, implying large plateaux. This same stability may be related with the achievable position resolution and in this sense one feels that only a proper control of the development of the streamer can lead to a significant improvement in position resolution that would make its applications much more important. Again the physical processes associated with the streamers, and most particularly the role played by photons are of special interest.

In the sequence of a previous paper¹ in which large plateaux were obtained using as additive benzene and triethylamine (possible fields of application would be related to UV detection), in this work we study the time evolution of the dead length and some characteristics of stability, in particular afterpulses development, and relate these data to some features associated with self-quenching streamers.

2. Experimental system

The experimental system used in this work is the same as described in ref. [1]. Essentially a proportional counter with a stainless steel cylindrical cathode 17 cm long and 4 cm diameter, and a nichrome wire 60 μm thick stretched along its axis. The bombarding radiation - X rays from a ⁵⁵Fe source - entered the chamber through a 10 mm diameter, 0.001" thick, beryllium window. The chamber was operated at atmospheric pressure in a continuous flow. Argon-isobutane in approximately 2:1 proportion (ratio of direct flowmeter readings) was used throughout this work. This proportion was kept even when a photoionizing vapour was added. The composition of the gas filling was achieved by mixing pure argon and isobutane with argon saturated with the photoionizing vapour.

3. Experimental results3.1 Afterpulses experimental data

The anode current pulses, through a 50 ohm resistance, fed a fast timing filter amplifier, whose output was simultaneously observed in an oscilloscope and sent to a scaler through a discriminator to reject noise and eventually proportional pulses.

The stability of the chamber was studied as a function of the gas filling composition, namely for the following gas mixtures: argon(Ar)-isobutane(Iso), Ar-Iso-benzene(B) and Ar-Iso-triethylamine(TEA). The benzene concentrations used were 0.1%, 1.5%, 3.4% and 7%; TEA concentrations were 1.1% and 4.5%. To achieve the lowest concentration of benzene argon was bubbled through cooled liquid benzene.

The addition of the photoionizing vapour to the gas mixture has a decisive influence on the stability of operation of the chamber in the self-quenching-streamer mode, and the nature and percentage of that vapour defines the region of operation of the device.

After the initial rise of the singles rate curves, due to the transition between the proportional and the limited streamer pulse operation, the plateaux have a width that depends strongly on the gas filling composition, at the end of which a new increase is, in most cases, observed due to afterpulses generation. It must be pointed out that with pure Ar-Iso mixtures afterpulses generation occurs at relatively low applied voltages. With low B and TEA, in general, they appear only at much higher voltages; the plateau width increases from about 100 V for 2:1 Ar-Iso mixture, to more than 1400 V for Ar-Iso-7%B (ref. [1]).

Figures 1, 2 and 3 display a few representative situations concerning characteristics of the afterpulses at the same applied voltage of 4700 V. A few comments should be made:

- Fig. 1 shows the afterpulses generated in Ar-Iso. Fig. 1 b) where a larger time-scale has been used, shows that the afterpulses come in bunches relatively well time defined; the delay time between the primary pulses and the successive afterpulses is constant, ~500 ns, in agreement with previous observation of the same phenomena². This time corresponds approximately to the electron drift time across the counter radius, supporting the hypothesis that the mechanism responsible for the time defined afterpulses is the emission of secondary electrons from the cathode walls due to ultraviolet photons associated with the SQS.

- Among the mixtures studied, at the anode voltage being considered (4700 V), besides the Ar-Iso one, only for very low concentrations of benzene, <0.5%, time-localized afterpulses appear; no afterpulses, either from the walls or from the gas filling are observed for Ar-Iso-7%B.

- Fig. 2 shows a few afterpulses being produced at a very low concentration of benzene (0.1%). It is clear that, although an important fraction of them tend to develop in time defined bunches, like in Ar-Iso mixture, others arise between the main signal and the first bunch, and eventually between successive afterpulses, as can be seen in Fig. 2 a). Increasing slightly the benzene concentration, no bunches of afterpulses arise; instead, only a few pulses spreading in the first 500 ns after the main signal, are observed.

- A similar pattern is observed with TEA, as displayed in Fig. 3. This figure, for 1.1% TEA, also exhibits afterpulses formation but without time definition. They also appear within ~500 ns of the main signal and are not time defined. Then, they probably arise from photoionizing processes taking place in the gas filling itself, and not from photoelectric effect in the cathode wall.

3.2 Dead length evolution

The dead time characteristics associated with the SQS mode have been already investigated by some authors²⁻⁵. It is well established that a streamer discharge is limited only to small distances along the anode wire, which implies that, after the occurrence of a streamer, only the wire part where it was located remains blocked for some time; so, other streamers can be detected during that time if they develop in other regions of the wire. To characterize this particular type of behaviour we will consider the dead length of the wire, δ , and its variation with time. Other authors³ defined a dead zone as the product of the blocked portion of the wire by the time it is blocked. Values for this last parameter, which depends on the gas mixture, are in the range of a few tens to a few hundreds $\mu\text{s}\cdot\text{cm}$: for a mixture of 50% argon + 33% methane + 17% methylal, $30 \mu\text{s}\cdot\text{cm}$ ⁴; for 70% argon + 28% isobutane + 2% methylal, $330 \mu\text{s}\cdot\text{cm}$ ⁵.

As it would be expected the value of δ decreases with the time. The time dependence of δ was studied by Alekseev et. al³ using a delayed self-coincidence method proposed by Kuptsov. In the present work we also investigated the time structure of δ and its dependence on the gas mixture and on the applied voltage, which, apart from its instrumental interest may provide information on the mechanisms of the SQS development.

In our study the frequency distribution of the time intervals between two consecutive streamers was determined and analyzed. This was accomplished by branching the output of the fast amplifier into two channels: one goes directly to the stop input of a time to amplitude converter, TAC, and the other is delayed and goes to the start input of the same unit. The output of the TAC is fed into a multichannel analyzer. Provided that the delay introduced is negligible compared to the mean interval between pulses, the output of the TAC will have an amplitude proportional to the time interval between two successive streamer pulses. Using convenient time delays obtained by a set of delay units (Ortec 416A Gate and Delay Generators) the time calibration of the system was made for all the time ranges of the TAC.

Time spectra were recorded for the different gas mixtures under study and for different anode voltages.

In the absence of dead time it is easy to show that the time distribution referred above would be described by a decreasing exponential with a decay constant that is the mean streamer rate. All the experimental spectra display this behaviour: except for the smaller times, the spectra plotted in a semilog scale are well fitted by a straight line with a slope that, within the experimental error, agrees with the measured streamer counting rate. The initial deviation from the straight line observed for the smaller time intervals is the result of losses due to the existence of the dead length. For those smaller times where dead time losses occur the relative loss in each channel was calculated by

$$(N_i^C - N_i^m) / N_i^C = L(t_i) \quad (1)$$

where t_i is the time corresponding to channel i and N_i^m and N_i^C are, respectively, the measured counts and the corrected counts in the same channel. For most of the distributions N_i^C is obtained by extrapolating the straight line fitted to the longer time region of the distribution where the dead time influence is negligible, (Fig. 4 a). For those distributions where the dead length remains significant even for the longer times, (Fig. 4 b), N_i^C was calculated using the experimental results obtained with a longer time range of the TAC, for the same mixture and anode voltage, after a proper correction due to the time calibrations of both ranges.

Clearly the relative loss observed in each channel is a function $f(\delta)$ at the corresponding time. The form of this function is dependent on the geometry of the

collimated beam for the bombarding radiation. It can be easily obtained for a rectangular window as it is the case in ref. [3] but not for a circular window as in our detector.

Let us assume a uniform rate irradiation through the entrance window and such that the dead time length is due to only one streamer discharge at a time. Both these hypothesis are well fulfilled by the long length of the collimator arrangement and the slow counting rate used. Events associated with the dead length, i.e., clusters of electrons migrating to this region of the wire, are assumed to produce no streamers; otherwise a full streamer is assumed to develop. Also diffusion effects of the electron cloud were neglected. In view of the dimensions of the collimator, R , and the range of δ , for smaller times $\delta \sim R$ (ref. [3]), care should be taken concerning dead lengths that extend outside the radius of the bombarding beam. This effect was also taken into account. It is a simple geometric problem now to establish a relationship between the percentage of losses and the dead length, i.e., $f(\delta)$. The computed results are displayed in Fig. 5. Based on these results and on the experimental values of the percentage of losses, $L(t)$ (eq. 1), the values of the dead length δ were plotted as a function of time for different mixtures and anode voltages. To those data we tentatively fitted exponentially decaying curves, $\delta = \delta_0 \exp(-t/\tau)$, which gave quite reasonable χ^2 . The parameters δ_0 and $t_{1/2} (= \ln 2 \cdot \tau)$ seem then to be a good choice to characterize the time structure of the dead length. Fig. 6 a) and b) shows some representative examples; solid lines represent the best fits obtained in each case.

Table 1 displays the values of these two parameters for the cases studied, together with other pertinent information. Typical errors are indicated in some cases.

Table 1

Gas mixture	Anode voltage (volt)	Charge Q (pC)	$t_{1/2}$ (μs)	δ_0 (mm)
Ar-Iso	4200	42	21 ± 3.5	$5.9^{+1.3}_{-0.9}$
Ar-Iso-4.5% TEA	4100	28	31^{+14}_{-8}	$4.4^{+1.2}_{-1.0}$
	4500	46	23 ± 3.5	8.2 ± 1.0
Ar-Iso-1.5% B	4300	54	$20^{+3.5}_{-2.0}$	8.6
Ar-Iso-3.4% B	4300	42	21	8.3
Ar-Iso-7% B	4100	26	49^{+14}_{-7}	4.0 ± 1.0
	4200	29	25 ± 3	7.5 ± 0.5
	4300	34	21 ± 3.5	8.3
	4700	50	15 ± 2	11.0 ± 1.5

4. Discussion

Though it is not possible, at this stage, to account for the origin of the photons responsible for the afterpulses or for the dependence of the spectral distribution of the emission on the applied high voltage, as this in an almost open field, a few general comments can nevertheless be made:

Afterpulse formation in pure Ar-Iso mixtures at the large isobutane concentrations used (>28.5%)¹ seems to imply that the photons responsible for this

effect must be beyond the isobutane absorption cut-off, i.e., $\lambda > 1640 \text{ \AA}$ (7.56 eV) and below the photoelectric threshold of the wall, i.e., $\lambda < 2700 \text{ \AA}$ (4.6 eV). Under the simplistic assumption that neither TEA nor B alter significantly the SQS, then those photons must be strongly absorbed by either TEA and B, which would explain their efficiency as stabilizers (TEA cut-off occurs at about 2500 \AA (4.96 eV)^{9,9} and B cut-off occurs at $\sim 2700 \text{ \AA}$ (4.59 eV)¹⁰⁻¹²).

Fig. 7 displays photoabsorption cross-sections σ for Iso, B and TEA as a function of wavelength, as found in the literature. The values for B and TEA are taken from the liquid phase, but they shouldn't be very different in the vapour phase. It is clear from the figure that, besides the total lack of information on some spectral regions, the agreement between the values of σ for TEA taken from different references is far from reasonable. Nevertheless, from the observed stabilizing effect of TEA and B, as already described, and from Fig. 7, the region 1700–2000 \AA appears as a reasonable guess for the photons responsible for the afterpulses originating from the walls.

In fact, in that region, benzene absorbs very strongly. Assuming an average value for $\bar{\sigma} \sim 50 \text{ Mb}$, the mean free path will be $\sim 0.5 \text{ mm}$ for 1.5% B and $\sim 8 \text{ mm}$ for 0.1% B. This means that, for the first concentration the photon beam intensity at the wall is reduced to about 10^{-17} of its initial value at the anode wire, while at 0.1% B that reduction is only of about 10^{-1} . So, if the photons responsible for the effect lie on that wavelength region, the stabilizing effect of benzene could be understood.

As far as TEA is concerned, the uncertainties in σ make the analysis more difficult. Assuming, in the same spectral region, an average value $\bar{\sigma} \sim 60 \text{ Mb}$ (curve 2 of Fig. 7), the mean free path will be $\sim 0.6 \text{ mm}$ for 1.1% and 0.15 mm for 4.5%, which gives a total light attenuation at the wall. If an average value of $\bar{\sigma} \sim 7 \text{ Mb}$ is assumed (curve 6 of Fig. 7), the attenuation of the beam will $\sim 10^{-2}$ and 10^{-7} , respectively. The former values seem to agree better with the observed results of the TEA addition.

It seems then likely that the photons responsible for the afterpulses originating from the cathode wall have wavelengths on that region. However, the observed fact that, for low TEA or B amounts and for very high voltages, a few afterpulses occur originating from the gas filling, means that, at least a few photons of $\lambda < 1653 \text{ \AA}$ (7.50 eV) and $\lambda < 1324 \text{ \AA}$ (9.24 eV), respectively, must be present.

Because the quantum efficiency of B and TEA in the region 1350–1100 \AA and 1600–1300 \AA , respectively, is high, a few photons could start the process. TEA ionization potential lies at a wavelength where absorption by isobutane is low, so this process could, in principle, be understood. However, assuming the values of σ of Fig. 7, afterpulses originating from the ionization of benzene are not understandable, as isobutane absorption is much higher in that region (both σ and the concentration are much higher). Of course another competitive mechanism could be one of radiationless energy transfer between the excited states responsible for the emission of those photons producing the afterpulses and appropriate levels of additives. At this stage this is unknown.

It must be also kept in mind that, besides the emission from highly excited argon atoms, formed upon recombination of Ar^+ plus electrons, there may be other emitting species, namely radicals from the broken isobutane chain. Some experimental evidence for such species in Ar/CH_4 mixtures has been reported⁷. Also we do not know in what extent, if any, the applied high voltage alters the spectral distributions of the emitted light.

Fig. 8 correlates δ_0 with the corresponding charge value, Q , for the several mixtures studied, and $1/\tau$ is displayed versus the high voltage, for the same mixtures in Fig. 9. The correlation shown in Fig. 8 is quite clear and reveals a feature that, in general terms, would be expected, namely that δ_0 increases with Q . However the experimental errors together with the number of data points associated with each mixture do not allow an exact determination of the relationship. The increase of δ_0 with Q can somewhat be supported by the data in Fig. 6 of ref. [3]. Also from Fig. 8, some dependence on the type of mixture is detected.

The time decrease of the dead length depends mostly on the mobility of the positive ions and in very general terms one would expect then an increase of τ^{-1} with the electric field. The electric field around the wire depends on the high voltage and on the streamer charge distribution but its mean value on that region increases with the high voltage, and then when this parameter increases $1/\tau$ should also increase. This behaviour, see Fig. 9, is not so clear as the previous one concerning Fig. 8, but some kind of agreement is found.

Acknowledgments

We thank Mr. Cidelio Cruz for his technical contribution and Mrs. Teresa H.V.T. Dias for computational help. Financial support from Instituto Nacional de Investigaao Cientıfica – Centro de Fısica da Radiaao e dos Materiais da Universidade de Coimbra – is acknowledged. We are indebted to the Deutscher Akademischer Austauschdienst and the Deutsche Gesellschaft fur Technische Zusammenarbeit.

References

- [1] E.P. de Lima, M. Saletto S.C.P. Leite, A.J.P.L. Policarpo and M.A.F. Alves, "Self-quenching streamers in mixtures with photoionization vapours", *IEEE Trans. Nucl. Sci.*, NS-30, pp. 90–94, 1983.
- [2] G. Battistoni, E. Iarocci, M.M. Massai, G. Nicoletti and L. Trasatti, "Operation of limited streamer tubes", *Nucl. Instr. and Meth.*, 164, pp. 57–66, 1979.
- [3] G.D. Alekseev, N.A. Kalinina, V.V. Karpukhin, D.M. Khazins and V.V. Kruglov, "Investigation of self-streamer discharge in a wire chamber", *Nucl. Instr. and Meth.*, 177, pp. 385–397, 1980.
- [4] G.D. Alekseev, N.A. Kalinina, V.V. Karpukhin, D.M. Khazins and V.V. Kruglov, "On a high current mode of wire chamber performance", *Nucl. Instr. and Meth.*, 153, pp. 157–159, 1978.
- [5] S. Brehin, A. Diamant Berger, G. Marel, G. Tarte, R. Turlay, G. Charpak and F. Sauli, "Some observations concerning the construction of proportional chambers with thick sense wires", *Nucl. Instr. and Meth.*, 123, pp. 225–229, 1975.
- [6] W. Braunschweig, "Spark Gaps and Secondary Emission Counters for Time of Flight Measurements", *Physica Scripta*, 23, pp. 384–392, 1981.
- [7] T.J. Sumner, G.K. Rochester, P.D. Smith, J.P. Cooch and R.K. Sood, "Scintillating drift chambers – The nature of the emission process in Ar/CH_4 ", *IEEE Trans. Nucl. Sci.*, NS-29, pp. 1410–1413, 1982.
- [8] Eileen Tannenbaum, Esther M. Coffin and Anna J. Harrison, "The far ultraviolet absorption spectra of simple alkyl amines", *J. Chem. Phys.*, 21, pp. 311–318, 1953.
- [9] Demis F. Grosjean and Peter Bletzinger, "Photoionization and photoabsorption characteristics of laser seed compounds", *IEEE J. Quantum Electron.*, QE-13, pp. 898–904, 1977.

- [10] I.B. Berlman, Handbook of Fluorescence Spectra of Aromatic Molecules, New York and London: Academic Press, 1971, ch. 6, pp. 108.
- [11] R.E. Dodd, Chemical Spectroscopy, Amsterdam - New York: Elsevier Publishing Company, 1962, ch. 4, pp. 227.
- [12] Charles L. Braun, Shunji Kato and Sanford Lipsky, "Internal conversion from upper electronic states to the first excited singlet state of benzene, toluene, p-xylene and mesitylene", J. Chem. Phys., 39, pp. 1645-1652, 1963.
- [13] A. Breskin, A. Cattai, G. Charpak, A. Peisert, A. Policarpo and F. Sauli, "Advance in vacuum ultra-violet detection with multi step gaseous detectors and application to Cerenkov ring imaging", IEEE Trans. Nucl. Sci., NS-28, pp. 429-439, 1981.
- [14] J. Seguinot and T. Ypsilantis, "Photo-ionization and Cerenkov ring imaging", Nucl. Instr. and Meth. 142, pp. 377-391, 1977.

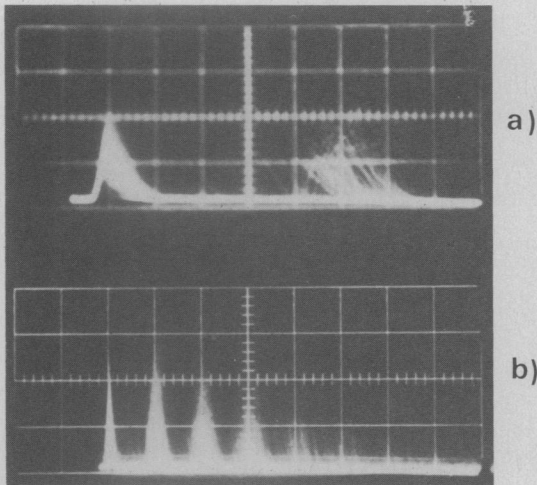


Fig. 1. Oscillograms of the current signals from the detector in the SQS-mode, showing primary pulses and localised afterpulses in the Ar-Iso mixture at 4700 V. Time scales: a) 0.1 $\mu\text{s}/\text{div}$; b) 0.5 $\mu\text{s}/\text{div}$.

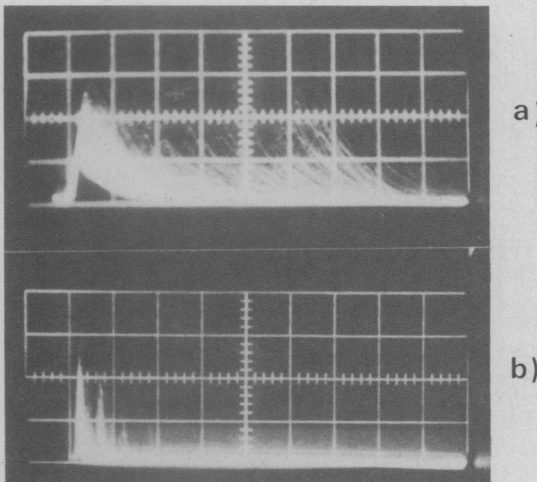


Fig. 2. Oscillograms of the current signals from the detector in the SQS-mode, showing primary pulses and afterpulses in the Ar-Iso-0.1% B at 4700 V. Time scales: a) 0.1 $\mu\text{s}/\text{div}$; b) 1 $\mu\text{s}/\text{div}$.

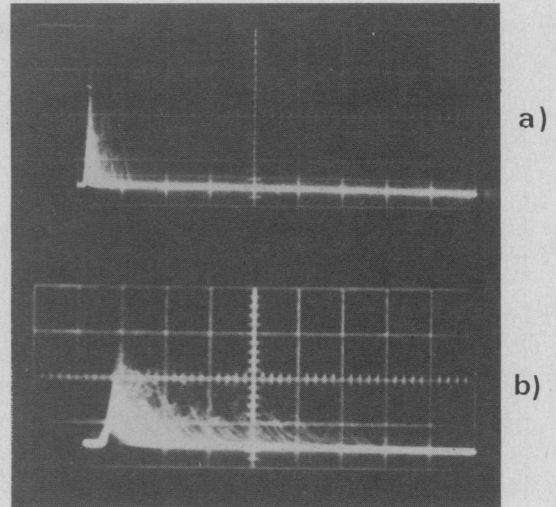


Fig. 3. Oscillograms of the current signals from the detector in the SQS-mode, showing primary pulses and afterpulses in the Ar-Iso-1.1% TEA at 4700 V. Time scales: a) 0.5 $\mu\text{s}/\text{div}$; b) 0.1 $\mu\text{s}/\text{div}$.

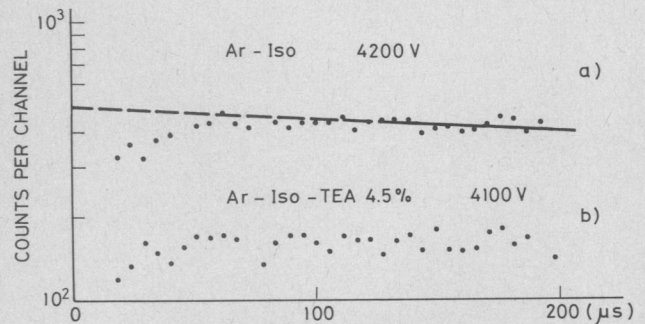


Fig. 4. Frequency distributions of the time intervals between two consecutive streamers: a) For the Ar-Iso mixture at 4200 V; a straight line is fitted to the points corresponding to $t_1 > 129 \mu\text{s}$; b) For a Ar-Iso-4.5% TEA at 4100 V.

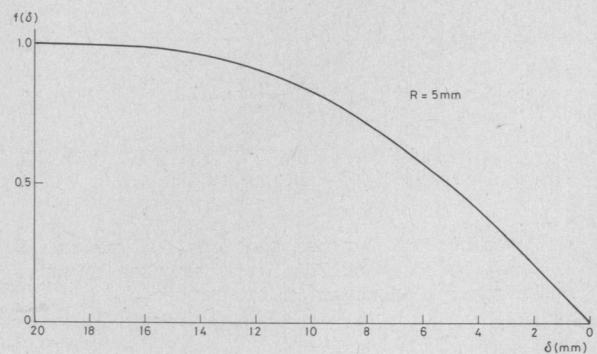


Fig. 5. The function $f(\delta)$ computed for a 5 mm radius circular window.

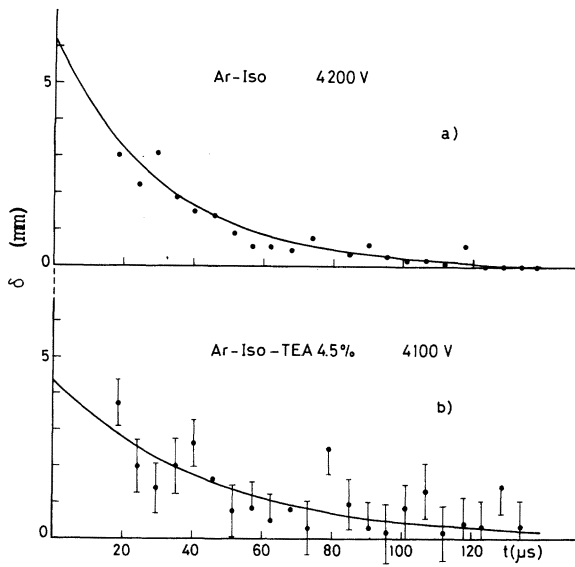


Fig. 6. Experimental values of the dead length δ plotted as a function of time: a) For the Ar-Iso mixture at 4200 V; b) For Ar-Iso-4.5%TEA at 4100 V

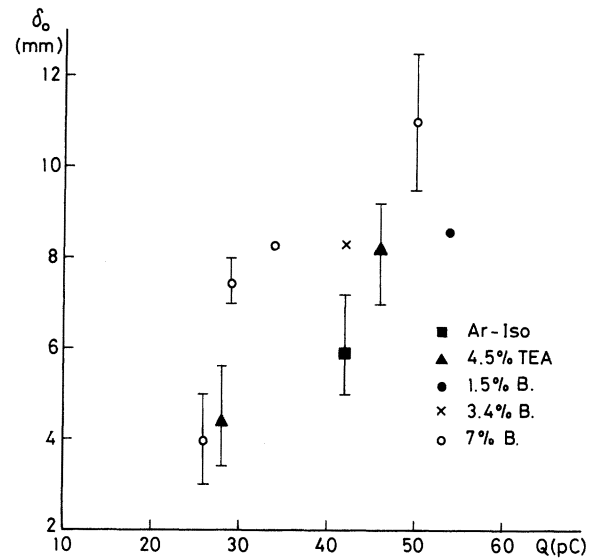


Fig. 8. Correlation between δ_0 and the charge Q developed in the streamer, for argon-isobutane, argon-isobutane-TEA and argon-isobutane-benzene mixtures in the percentages indicated.

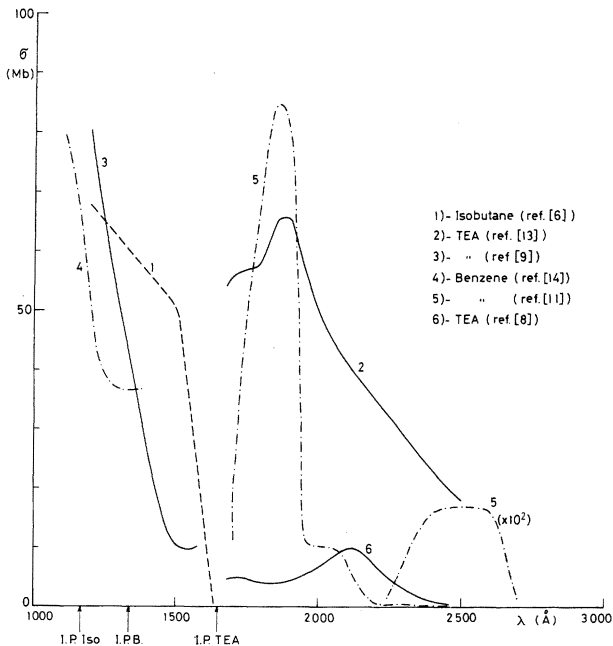


Fig. 7. Photoabsorption cross sections, σ , for isobutane, benzene and TEA, as a function of wavelength, λ , as found in literature.

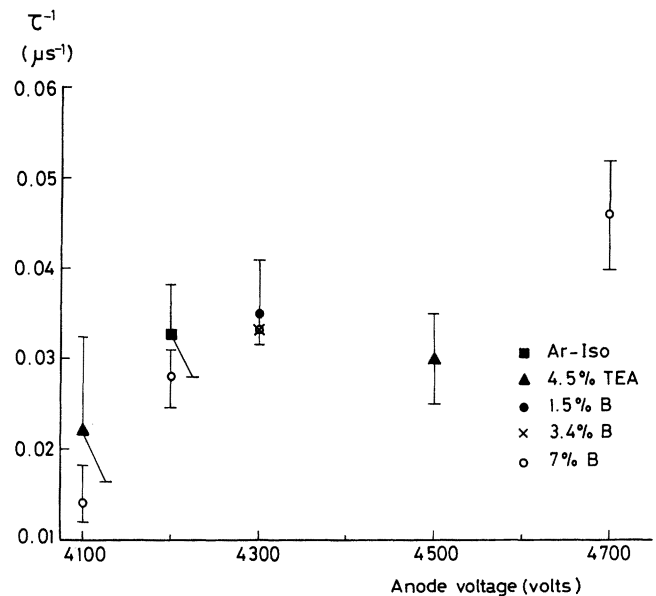


Fig. 9. Correlation between τ^{-1} and the anode voltage for different gas fillings.